

Chapter 21

Electrochemical X-Ray Photoelectron Spectroscopy

Takuya Masuda

Keywords Electrochemistry · Solid/liquid interfaces · In situ X-ray photoelectron spectroscopy

21.1 Principle

Although X-ray photoelectron spectroscopy (XPS) requires a vacuum (Chap. 132 X-ray Photoelectron Spectroscopy), in situ electrochemical (EC-) XPS has been a long-standing dream not only for fundamental science, but also for a wide range of applications including fuel cells, rechargeable batteries, photocatalysts, and biological processes. To date, as shown in Fig. 21.1, three approaches enabling in situ EC-XPS have been successfully reported by using near-zero vapor pressure room temperature ionic liquids (RTILs) as an electrolyte solution [1], a near-ambient pressure (NAP-) XPS equipped with a differential pumping system [2, 3], and an environmental cell with an ultrathin membrane-type working electrode [4, 5].

21.2 Features

- Elemental composition at the solid/liquid interface can be determined under electrochemical potential control, as well as the oxidation state of each element.
- Surfaces of an ionic liquid, an electrode and their boundary can be measured under electrochemical potential control by using an ionic liquid as an electrolyte solution in vacuum.

T. Masuda (✉)

Research Center for Advanced Measurement and Characterization,
National Institute for Materials Science (NIMS), Tsukuba,
Ibaraki 305-0044, Japan
e-mail: MASUDA.Takuya@nims.go.jp

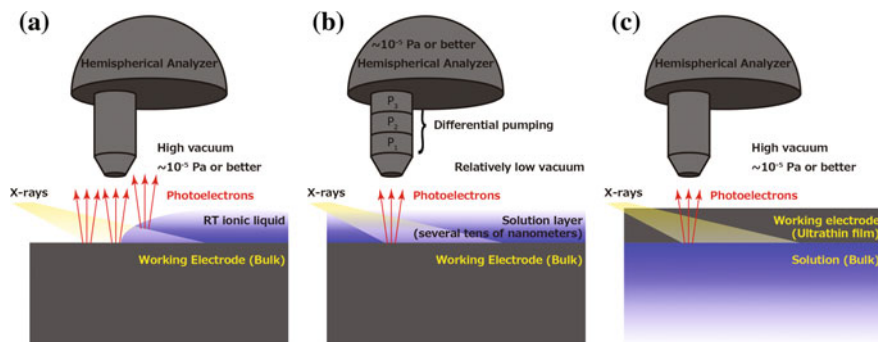


Fig. 21.1 Schematic illustrations of in situ EC-XPS using **a** RTILs, **b** NAP-XPS, and **c** environmental cells with an ultrathin membrane-type working electrode

- Electrode surfaces can be measured through a thin solution layer by utilizing a differential pumping system with an electrostatic lens.
- Electrode surfaces in contact with a bulk solution can be measured through an ultrathin membrane-type working electrode which is also used as a separator between vacuum and the ambient.

21.3 Instrumentation

An electrochemical cell consisting of RTILs as an electrolyte solution and working and reference/counter electrodes (Fig. 21.2a) can be directly introduced into a vacuum chamber. XPS measurements of the surfaces of the RTIL droplet and the working electrode can be taken under electrochemical potential control.

In NAP-XPS, samples placed under a relatively low vacuum can be measured by utilizing a differential pumping system and electrostatic lens (as described in Chap. 3 Ambient Pressure X-ray Photoelectron Spectroscopy) [6, 7]. In this method, electrodes partially withdrawn from the electrochemical cell can be measured in the presence of a thin liquid layer under electrochemical potential control, by detecting photoelectrons emitted from the electrode surface through the liquid layer (Fig. 21.2b). The thickness of the liquid layer is limited to the range from several nanometers to several tens of nanometers by the inelastic mean free path of photoelectrons in the liquid layer and can be controlled by relative humidity and temperature.

By using an environmental cell, in which an ultrathin membrane is used as a window for X-rays and photoelectrons, a separator between vacuum and liquid, and a working electrode for electrochemical reactions, XPS measurements of the electrode surface in the presence of a “filling” thick liquid layer can be performed

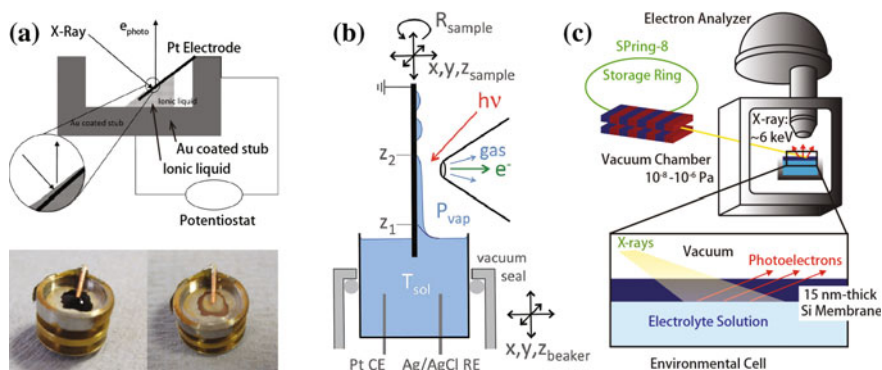


Fig. 21.2 Experimental setups for in situ EC-XPS using **a** RTILs [8, 9], **b** NAP-XPS [3], and **c** environmental cells with an ultrathin membrane-type working electrode [4]

by detecting photoelectrons emitted from the solid/liquid (membrane/liquid) interface through the membrane (Fig. 21.2c).

21.4 Applications

21.4.1 EC-XPS Utilizing RTILs [9, 10]

Figure 21.3a shows a time course of XPS spectra in the Cu 2p region taken during the potentiostatic electrolysis of a Cu electrode at +1.8 V in (N-methylacetate)-4-picolinium bis(trifluoromethylsulfonyl)imide [MAP][Tf₂N] [9]. The surface of a [MAP][Tf₂N] droplet at 2.2 mm from the electrode surface was measured in the snapshot mode. A peak due to the Cu 2p_{3/2} was observed from the third scan and the intensity gradually increased up to the eighth scan, suggesting that the Cu⁺ ions electrochemically dissolved from the Cu electrode in the ionic liquid and diffused to the analysis point.

Figure 21.3b shows another example of the EC-XPS utilizing RTILs. In this report, the surface of a Ni mesh electrode was measured during the galvanostatic electrolysis at -1×10^{-5} A in N-butyl-N-methylpyrrolidinium bis(trifluoromethylsulfonyl)imide [C₄mpyr][NTf₂] containing 0.1 M Rb[NTf₂] [10]. A peak due to the Rb 3d clearly increased with time because of the electrochemical deposition of Rb on the Ni mesh electrode. Thus, the EC-XPS using RTILs is capable of chemical analysis and mass transport analysis during the electrochemical reactions.

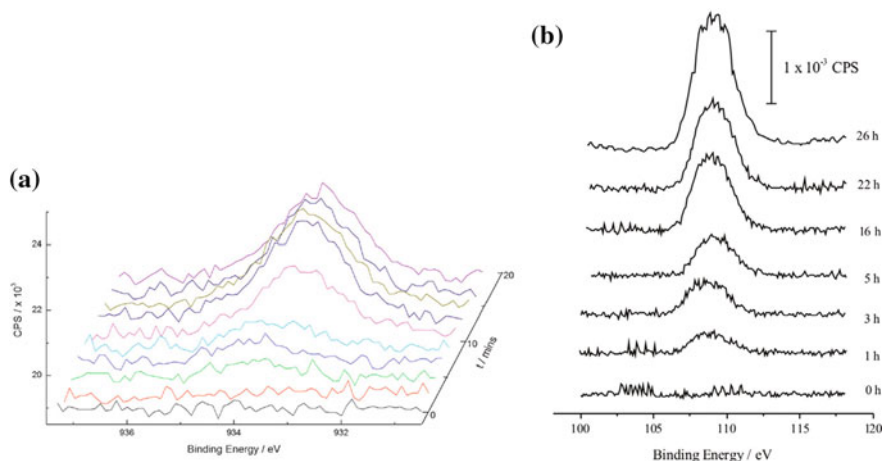


Fig. 21.3 Time courses of XPS spectra in **a** the Cu 2p region at a surface of [MAP][Tf₂N] droplet during the electrolysis of Cu electrode at +1.8 V (vs. Mo stub) [9] and **b** the Rb 3d region at a Ni mesh electrode during the electrolysis at -1×10^{-5} A in [C₄mpyrr][NTf₂] containing 0.1 M Rb [NTf₂] [10]

21.4.2 EC-XPS Utilizing NAP-XPS [11]

Figure 21.4a, b shows XPS spectra in the N 1s and O 1s regions of a Au electrode measured at various potentials in an aqueous solution of 1 M pyrazine plus 0.4 mM KOH in the configuration shown in Fig. 21.2b. In the N 1s region, two peaks corresponding to pyrazine molecules adsorbed on the electrode (Py_{ESF}) and solvated in the liquid phase (LPPy) were observed at 399.7 eV and a higher binding energy, respectively. In the O 1s region, three components attributed to water molecules in gas (GPW) and liquid phases (LPW) and adsorbed hydroxyl groups were observed. When the potential was made more negative (positive) from open circuit potential, *ca.* 150 mV, the peak positions for water molecules (LPW) and pyrazine in the liquid phase (LPPy) shifted to the higher (lower) binding energy although those for the adsorbed pyrazine (Py_{ESF}) and hydroxyl groups did not shift. In addition, the width of the peaks corresponding to the solution species such as LPW and LPPy significantly changed possibly due to the potential distribution across the electrical double layer (EDL). As shown in Fig. 21.4c and d, the minimum point of the double-layer capacitance coincides with that of the peak width at the potential of zero charge (PZC) at which the electrical charge on the electrode surface is zero. Thus, the EC-XPS using a NAP-XPS system enables to probe the potential distribution across the EDL although its very thin solution layer may cause a high cell resistance.

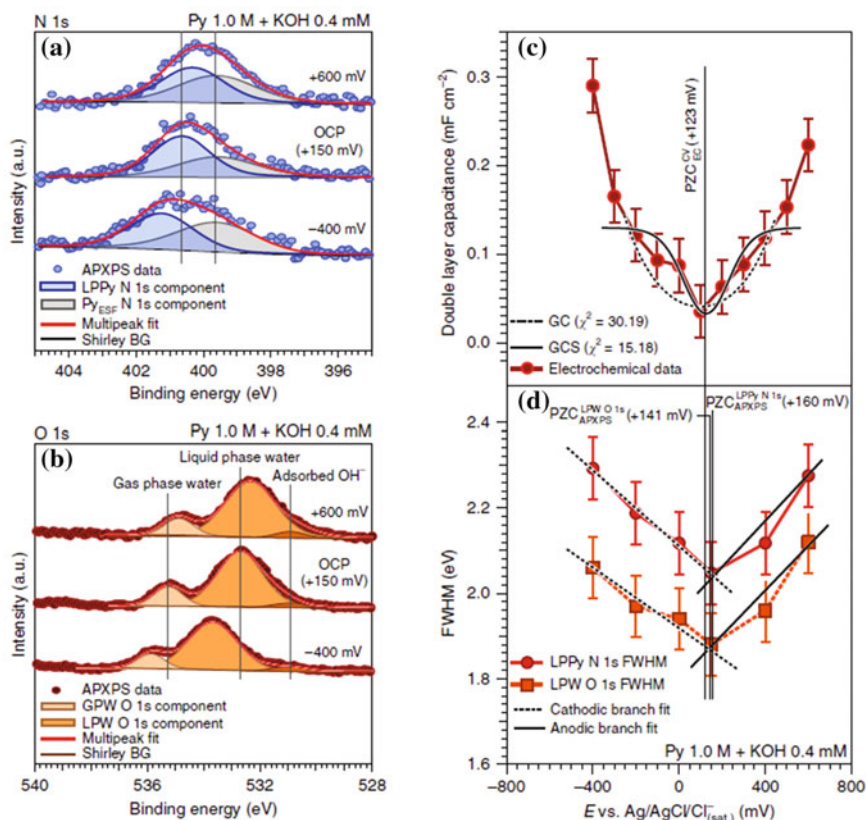


Fig. 21.4 XPS spectra in **a** the N 1s and **b** the O 1s regions of a Au electrode measured at various potentials in an aqueous solution of 1 M pyrazine plus 0.4 mM KOH in the configuration shown in Fig. 21.2b [11]. **c** Double-layer capacitance obtained from electrochemical measurements by using both Gouy–Chapman (GC) and Gouy–Chapman–Stern (GCS) models and full-width at half-maximum (FWHM) of LPPy N 1s and LPW O 1s peaks as a function of the applied potential [11]

21.4.3 EC-XPS Utilizing an Environmental Cell [4]

An environmental cell with an ultra-small volume was utilized for the ‘first’ in situ EC-XPS experiment in an ordinary solvent to prevent any possible damage caused by breakage of the ultrathin Si membrane-type working electrode used as a separator between vacuum and the ambient (Fig. 21.5a). In this configuration, anodic current started to flow from *ca.* 0.8 V only in the presence of water (Fig. 21.5b), implying the electrochemical growth of Si oxide. As shown in the EC-XPS spectra in Fig. 21.5c–d, not only doublet peaks at 100 and 99.5 eV corresponding to Si 2p_{1/2} and 2p_{3/2}, respectively, but also a broad peak at 104.5 eV corresponding to SiO₂

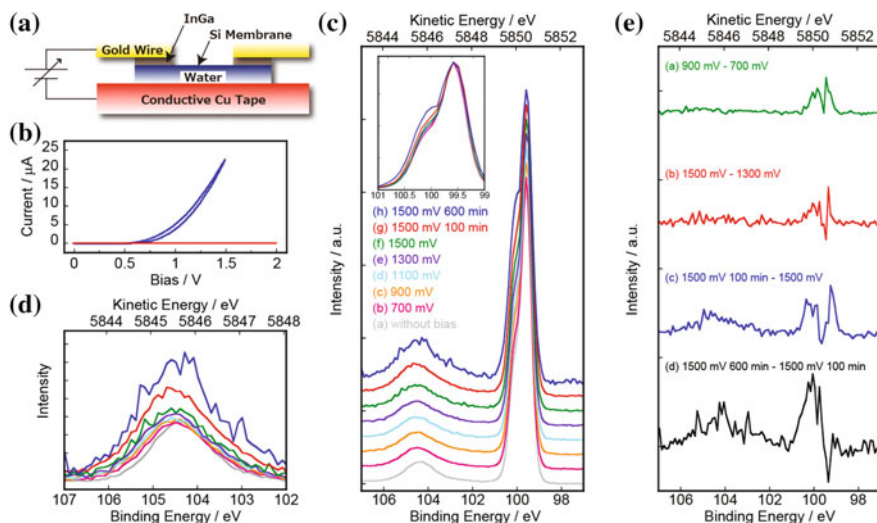


Fig. 21.5 **a** Schematic illustration and **b** I–V relationships of the environmental cell with (blue) and without water (red) [4]. **c** Photoelectron spectra in the Si 2p region of the Si membrane measured under various bias applications [4]. **d** Magnified image of (c) in the region between 107 and 102 eV, corresponding to SiO₂. **e** Difference spectra at various conditions [4]

was observed even without a bias application, suggesting the existence of native oxide. When a positive potential was applied to the Si membrane with respect to the Cu tape, the peak intensity due to the SiO₂ increased gradually, confirming the electrochemical growth of SiO₂ at the Si membrane/water interface. In addition, the ratio of Si 2p_{1/2} and 2p_{3/2} changed significantly, suggesting that strained Si atoms at the Si/Si oxide interface became closer to the analysis side, accompanying the electrochemical growth of SiO₂, as clearly indicated in the difference spectra (Fig. 21.5e). On the basis of the inelastic mean free paths of the Si 2p photoelectrons in Si oxide and Si obtained using the TPP-2 M formula and the atom densities of Si in Si oxide and Si, the thickness change of SiO₂ during the electrochemical growth was estimated in a sub-nanometer scale. The most difficult challenge of this technique is development of ultrathin films with very high conductivity and mechanical strength, which can be used as a membrane-type working electrode.

References

1. Lovelock, K.R.J., Villar-Garcia, I.J., Maier, F., Steinruck, H.P., Licence, P.: Photoelectron spectroscopy of ionic liquid-based interfaces. *Chem. Rev.* **110**, 5158–5190 (2010)
2. Axnanda, S., Crumlin, E.J., Mao, B.H., Rani, S., Chang, R., Karlsson, P.G., Edwards, M.O. M., Lundqvist, M., Moberg, R., Ross, P., Hussain, Z., Liu, Z.: Using “tender” X-ray ambient

- pressure X-ray photoelectron spectroscopy as a direct probe of solid-liquid interface. *Sci. Rep.* **5**, 9788 (2015)
3. Karslioglu, O., Nemsak, S., Zegkinoglou, I., Shavorskiy, A., Hartl, M., Salmassi, F., Gullikson, E.M., Ng, M.L., Rameshan, C., Rude, B., Bianculli, D., Cordones, A.A., Axnanda, S., Crumlin, E.J., Ross, P.N., Schneider, C.M., Hussain, Z., Liu, Z., Fadley, C.S., Bluhm, H.: Aqueous solution/metal interfaces investigated in operando by photoelectron spectroscopy. *Faraday Discuss.* **180**, 35–53 (2015)
 4. Masuda, T., Yoshikawa, H., Noguchi, H., Kawasaki, T., Kobata, M., Kobayashi, K., Uosaki, K.: In situ X-ray photoelectron spectroscopy for electrochemical reactions in ordinary solvents. *Appl. Phys. Lett.* **103**, 111605 (2013)
 5. Velasco-Velez, J.J., Pfeifer, V., Havecker, M., Weatherup, R.S., Arrigo, R., Chuang, C.H., Stotz, E., Weinberg, G., Salmeron, M., Schlögl, R., Knop-Gericke, A.: Photoelectron spectroscopy at the graphene-liquid interface reveals the electronic structure of an electrodeposited cobalt/graphene electrocatalyst. *Angew. Chem. Int. Ed.* **54**, 14554–14558 (2015)
 6. Ogletree, D.F., Bluhm, H., Lebedev, G., Fadley, C.S., Hussain, Z., Salmeron, M.: A differentially pumped electrostatic lens system for photoemission studies in the millibar range. *Rev. Sci. Instrum.* **73**, 3872–3877 (2002)
 7. Salmeron, M., Schlögl, R.: Ambient pressure photoelectron spectroscopy: a new tool for surface science and nanotechnology. *Surf. Sci. Rep.* **63**, 169–199 (2008)
 8. Taylor, A.W., Qiu, F.L., Villar-Garcia, I.J., Licence, P.: Spectroelectrochemistry at ultrahigh vacuum: in situ monitoring of electrochemically generated species by X-ray photoelectron spectroscopy. *Chem. Commun.* 5817–5819 (2009)
 9. Qiu, F.L., Taylor, A.W., Men, S., Villar-Garcia, I.J., Licence, P.: An ultra high vacuum-spectroelectrochemical study of the dissolution of copper in the ionic liquid (N-methylacetate)-4-picolinium bis(trifluoromethylsulfonyl)imide. *Phys. Chem. Chem. Phys.* **12**, 1982–1990 (2010)
 10. Wibowo, R., Aldous, L., Jacobs, R.M.J., Manan, N.S.A., Compton, R.G.: In situ electrochemical-X-ray photoelectron spectroscopy: rubidium metal deposition from an ionic liquid in competition with solvent breakdown. *Chem. Phys. Lett.* **517**, 103–107 (2011)
 11. Favaro, M., Jeong, B., Ross, P.N., Yano, J., Hussain, Z., Liu, Z., Crumlin, E.J.: Unravelling the electrochemical double layer by direct probing of the solid/liquid interface. *Nat. Commun.* **7**, 12695 (2016)